The Astrophysical Journal Letters, 913:L6 (5pp), 2021 May 20 https://doi.org/10.3847/2041-8213/abf836

Precovery Observations Confirm the Capture Time of Asteroid 2020 CD3 as Earth's Minimoon

Shantanu P. Naidu[1], Marco Micheli[2], Davide Farnocchia[1], Javier Roa[1], Grigori Fedorets[3], Eric Christensen[4], and Robert Weryk[5]
[1] Jet Propulsion Laboratory, California Institute of Technology, Pasadena, CA, 91109, USA; shantanu.p.naidu@jpl.nasa.gov
[2] ESA NEO Coordination Centre, Largo Galileo Galilei, 1, I-00044 Frascati (RM), Italy
[3] Astrophysics Research Centre, School of Mathematics and Physics, Queen's University Belfast, Belfast BT7 1NN, UK
[4] The University of Arizona, Lunar and Planetary Laboratory, 1629 E. University Boulevard,Tucson, AZ 85721, USA
[5] University of Hawai'i, Institute for Astronomy, 2680 Woodlawn Drive, Honolulu, Hawai'i, 96822, USA
Received 2021 February 25; revised 2021 March 31; accepted 2021 March 31; published 2021 May 18

Abstract

Asteroid 2020 CD3 was discovered on 2020 February 15 by the Catalina Sky Survey while it was temporarily captured in a geocentric orbit before escaping Earth's Hill sphere on 2020 March 7. We searched archival images and found precoveries of 2020 CD3 from the Dark Energy Camera and Catalina Sky survey. The Dark Energy Camera images yielded three observations on 2019 January 17, while the Catalina Sky Survey images yielded four observations on 2019 January 24 from the Mt. Lemmon telescope and four observations on 2018 May 9 from the Mt. Bigelow telescope. These precovery observations allowed us to refine the orbit of 2020 CD3 and determine that it was captured in a geocentric orbit on 2017 September 15 after a close approach to the Moon at a distance of $11{,}974 \pm 10$ km. We analyzed the trajectory of 2020 CD3 to look for potential Earth impacts within the next 100 years and find a $\gtrsim$1% probability of an impact between 2061 and 2120 depending on nongravitational force model assumptions. The small size of 2020 CD3, about 1 to 2 m, makes any potential impact harmless.

Unified Astronomy Thesaurus concepts: Near-Earth objects (1092); Asteroids (72)

1. Introduction

Asteroid 2020 CD3 was discovered by K. Wierzchoś and T. Pruyne at the Catalina Sky Survey Mt. Lemmon Station on 2020 February 15 and found to be on a geocentric orbit (MPEC 2020-D104).[6] Both astrometric and physical observations show that 2020 CD3 is a natural, meter-sized body (Fedorets et al. 2020), thus making it Earth's second discovered temporary satellite, or minimoon (Granvik et al. 2012; Fedorets et al. 2017), 14 years after the first one (2006 RH_{120}; Kwiatkowski et al. 2009, MPEC 2008-D12)[7]. This discovery confirms the existence of minimoons as a population (Jedicke et al. 2018) and the predicted observational interval of a decade with existing asteroid surveys (Bolin et al. 2014).

The spectral type of 2020 CD3 mostly resembles a V-type asteroid in terms of Bus-DeMeo taxonomy (Bolin et al. 2020). The V-type classification is consistent with the derived Monte Carlo distribution of density values of 2020 CD3, assuming albedoes typical for the V spectral class (Fedorets et al. 2020). While non-principal-axis rotation state could not be ruled out, the most plausible rotation period for 2020 CD3 is estimated to be 3 minutes and 10 s. The best estimate for the size of 2020 CD3, combining the brightness and spectro-photometric data, and phase curve fit yield the diameter of $1.2^{+0.4}_{-0.2}$ m. This size is further confirmed by the nondetection of 2020 CD3 by the Arecibo observatory radar. 2020 CD3 is probably a free-floating analog of a boulder found on surfaces of larger asteroids. As of early 2021, 2020 CD3 is 1 of the 10 smallest discovered asteroids, and among the best-characterized in the meter-size range, including the photometric colors, extensive astrometric coverage, and a photometric lightcurve. Therefore, it is an object of particular interest both in terms of its dynamics within the Earth–Moon system, as well as being a representative of a little-studied population of meter-size asteroids.

The astrometric and physical characterization data collected for asteroid 2020 CD3 provided a rare opportunity for investigating the detailed dynamical behavior of a natural body in Earth's vicinity for an extended period of time. The initial calculations by de la Fuente Marcos & de la Fuente Marcos (2020) and Bolin et al. (2020) indicated that 2020 CD3 has an exceptionally long geocentric capture. Fedorets et al. (2020) show that 2020 CD3 had been captured for at least 2.5 years, with a deterministic orbit of 2020 CD3 since the close approach with the Moon on 2017 September 15. However, the direct origin from the Moon as well as the capture scenario on a previous date could not be ruled out. Searches by Fedorets et al. (2020) in archival data from Pan-STARRS, Catalina Sky Survey, Zwicky Transient Facility, and China Near-Earth Object Survey Telescope did not yield any precovery detections of 2020 CD3 that could improve the orbital knowledge.

2. Precovery Observations

After the finalization of Fedorets et al. (2020), with the now complete 3 month observed arc for the 2020 apparition, we repeated a full search for possible precovery observations using the Solar System Object Image Search (SSOIS) made available by the Canadian Astronomy Data Centre (Gwyn et al. 2012). The system allows an ephemeris-based query of dozens of professional telescope archives, covering more than 50 telescope-instrument combinations.

We used our best-available ephemeris to investigate the existence of possible fields covering the expected position of 2020 CD3 from 2017 September 15 onward, with a particular focus on possible hits from large-FoV optical imagers such as Canada–France–Hawai'i Telescope's MegaCam and the Dark Energy Camera (DECam) instrument on the 4 m Blanco

[6] https://www.minorplanetcenter.org/mpec/K20/K20DA4.html
[7] https://www.minorplanetcenter.org/mpec/K08/K08D12.html

Table 1
Osculating Heliocentric Orbital Elements of 2020 CD3 and 1σ Uncertainties in the Ecliptic Frame for Various Models of Nongravitational Accelerations

Solution #	23	24	25	26
Eccentricity	0.011321553(13)	0.011321439(43)	0.011321447(39)	0.011321447(39)
Perihelion (au)	0.9782895316(22)	0.9782895212(43)	0.9782895203(45)	0.9782895205(45)
Perihelion time (TDB)	2458819.602684(18)	2458819.602525(66)	2458819.602547(51)	2458819.602547(51)
Longitude of node (°)	31.759580(31)	31.759414(68)	31.759380(77)	31.759377(78)
Argument of perihelion (°)	37.674030(24)	37.674034(46)	37.674090(32)	37.674093(33)
Inclination (°)	0.58581587(11)	0.58581626(18)	0.58581626(18)	0.58581625(19)
A_1 (10^{-10} au/d^2)	1.354(25)	1.578(83)	1.530(67)	1.599(91)
A_2 (10^{-10} au/d^2)	…	0.010(27)	…	…
A_3 (10^{-10} au/d^2)	…	−0.050(18)	…	…
A_{J_1} (10^{-10} au/d^2)	…	…	0.014(143)	0.15(13)
A_{J_2} (10^{-10} au/d^2)	…	…	0.32(11)	−0.21(18)
χ^2	104.8	96.9	96.5	96.6

Note. The osculating epoch is 2020 June 1.0 TDB. Solution 23 uses A_1, solution 24 uses A_1, A_2, and A_3, and solutions 25 and 26 use a rotating jet model with the best-fit retrograde and prograde poles, respectively.

Telescope. We then filtered the resulting hits on the basis of the expected signal-to-noise ratio (S/N) of a detection given the properties of the specific imager, and were left with five possible nights from 2018 February to 2019 January, during which the object could have produced a detection with S/N greater than 3, all from the DECam instrument.

We downloaded the corresponding exposures, and carefully inspected the area corresponding to the ephemeris uncertainty of 2020 CD3 by eye, in order to locate possible trailed detections. The analysis proved successful for a pair of g- and r-band exposures obtained on 2019 January 17 by the DECam Plane Survey: the 30 s *r*-band exposure contained a clear high-S/N trail, for which both trail ends could easily be measured, while the longer 96 s *g*-band trail contained a fainter and longer trail, truncated by the edge of the array, for which only one end could be measured.

The addition of the DECam precovery observations resulted in a much better knowledge of the prediscovery orbit for 2020 CD3, and consequently allowed us to produce a more accurate ephemeris, which we could use to repeat our search into the Catalina Sky Survey archive.

The refined search proved successful, allowing us to identify a set of detections on 2019 January 24 from the Mt. Lemmon telescope (G96), and even a further set as far back as 2018 May 9 from the Mt. Bigelow Schmidt (703).

The four images from the Mt. Lemmon telescope, although faint, could all be measured individually, and resulted in four separate astrometric measurements. The Mt. Bigelow ones, on the other hand, were significantly trailed, and therefore we could only measure five of the eight trail ends, while the remaining three were either too faint, or affected by field objects. We also used the improved orbit to search the Pan-STARRS image archive, but found no precovery detections.

3. Orbit

The extended arc of astrometric observations called for a highly accurate force model. We accounted for gravitational forces due to the Sun, planets, and the 16 most massive asteroids (Folkner et al. 2014; Farnocchia et al. 2015). For Earth's gravity, we used a 4×4 geopotential with spherical harmonics coefficients from the EGM96 geopotential model (Lemoine et al. 1998). It is worth pointing out that nonzonal coefficients were necessary to fit the data.

As shown by Fedorets et al. (2020), the motion of 2020 CD3 is significantly perturbed by solar radiation pressure (SRP). Similar to the Marsden et al. (1973) formulation, we modeled SRP as a purely radial acceleration A_1/r^2, where r is the heliocentric distance in au. JPL solution #23 in Table 1 lists the best-fit orbit solution based on this model. We used 126 optical observations spanning about two years between 2018 May 9 and 2020 May 21.

Asymmetries in the surface of the asteroid can cause the SRP to have nonradial components. Therefore, we added transverse and normal components to the nongravitational perturbation model A_2/r^2 and A_3/r^2, respectively. The A_2 parameter would also contain a signal from the Yarkovsky drift; however, this contribution should be negligible over such a short timespan. The best-fit orbit solution using this model is listed in Table 1 (solution #24). As indicated by the χ^2 values, this model only leads to a marginal improvement in the fit relative to the A_1-only model (solution #23). However, it leads to larger and likely more realistic uncertainties.

The Marsden et al. (1973) nongravitational model is expressed in the radial-transverse-normal frame and so is tied to the heliocentric orbit of 2020 CD3, which is not optimal given that the object is captured by the Earth. Since the nonradial components of solar radiation forces are tied to the surface topography and physical properties, they effectively behave like jets that are fixed at certain locations on the asteroid with strength proportional to $1/r^2$. Therefore, we considered the rotating jet model (RJM; Chesley & Yeomans 2005) with a $1/r^2$ dependence, in addition to the main radial term. The RJM is tied to the body-fixed frame and so is suitable to capture asymmetries in SRP.

We assumed two jets on the surface of the asteroid, one at a high latitude of 80° and another at a mid-latitude of −45°, similar to what was done in Chesley & Yeomans (2005). Then, performed a raster scan for the spin pole of the asteroid: we fixed the spin pole at various orientations and estimated A_1, A_{J_1}, and A_{J_2}. Figure 1 shows the χ^2 countour levels as a function of the spin pole of the asteroid. Two local minima, centered on (R. A., decl.) of (70,−50)° and (250, 50)°, are visible. The estimated parameters of the RJM for these spin poles are listed in Table 1 as solutions #25 and #26, respectively. Also the RJM only provides a marginal improvement in the fit.

For the four solutions in Table 1 we analyzed the past trajectory of 2020 CD3 using a Monte Carlo approach. Thanks

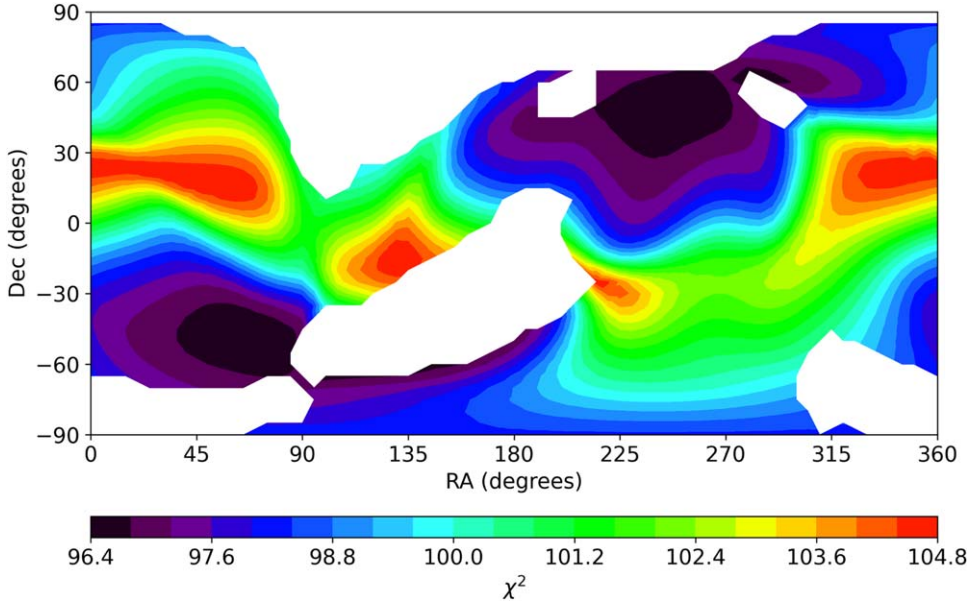

Figure 1. Contour plot of χ^2 as a function of asteroid spin pole used in the rotating jet model. White areas are regions where the fits did not converge.

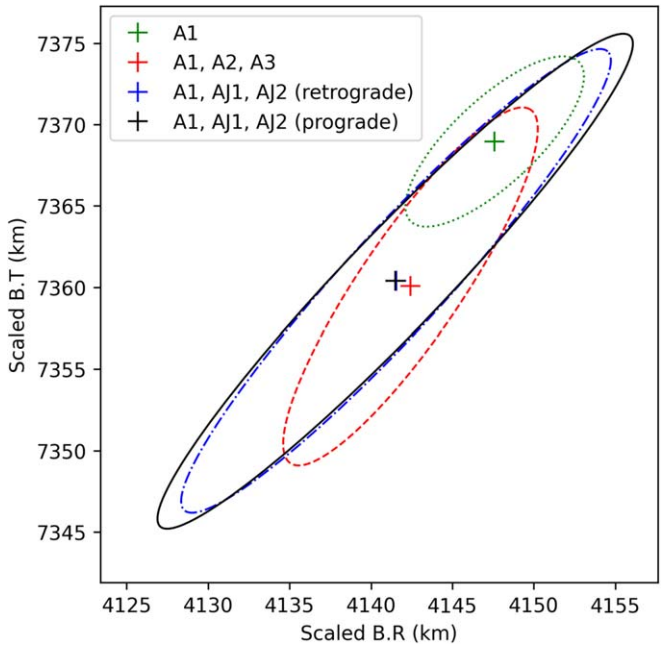

Figure 2. 2020 CD3 trajectories and 3σ uncertainties corresponding to solutions in Table 1 mapped onto the outbound scaled B-plane (Farnocchia et al. 2019) of the Moon on 2017 September 15. All trajectories are captured on a geocentric orbit during this encounter corresponding to the blue samples in Figure 4(a) of Fedorets et al. (2020).

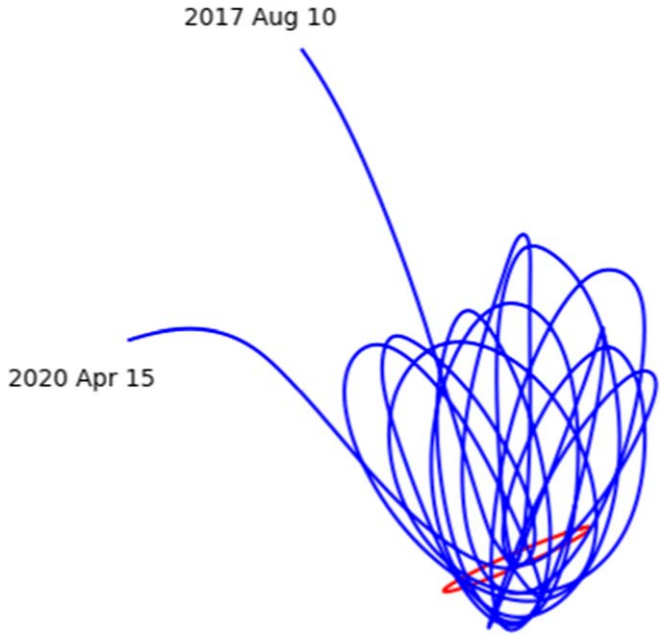

Figure 3. Trajectory of 2020 CD3 (blue) relative to the Earth (not seen), as seen from the $+x$ equatorial J2000 axis. The orbit of the Moon is shown in red for scale.

to the precovery data, the circumstances of the lunar encounter on 2017 September 15 are now determined. All four trajectories make a close approach to the Moon on 2017 September 15.1837 TDB $\pm$ 0.0002 days at a distance of 11,974 $\pm$ 10 km and are captured into a geocentric orbit after this encounter. Figure 2 shows the mapping of the different solutions onto the B-plane of the Moon (Farnocchia et al. 2019). All solutions predict consistent close approach distances and times within 3σ. This result rules out the lunar origin or earlier capture scenarios that were possible in Fedorets et al. (2020). 2020 CD3 stayed in a geocentric orbit for about 2.5 years before exiting Earth's Hill sphere ($\sim$0.01 au) on 2020 March 7. Figure 3 shows the trajectory of 2020 CD3 around this time and Figure 4 shows the trajectory plotted over the residence time of simulated minimoons.[8]

4. Future Impact Probability

To assess the impact probability of the four solutions listed in Table 1, we ran Monte Carlo simulations with 10^6 samples to detect virtual impactors (VIs) through 2120 November. The

[8] We note that there is an error in similar plots in Granvik et al. (2012), Fedorets et al. (2017), and Jedicke et al. (2018). The plots in the these articles plot perihelion distance on the x-axis instead of semimajor axes.

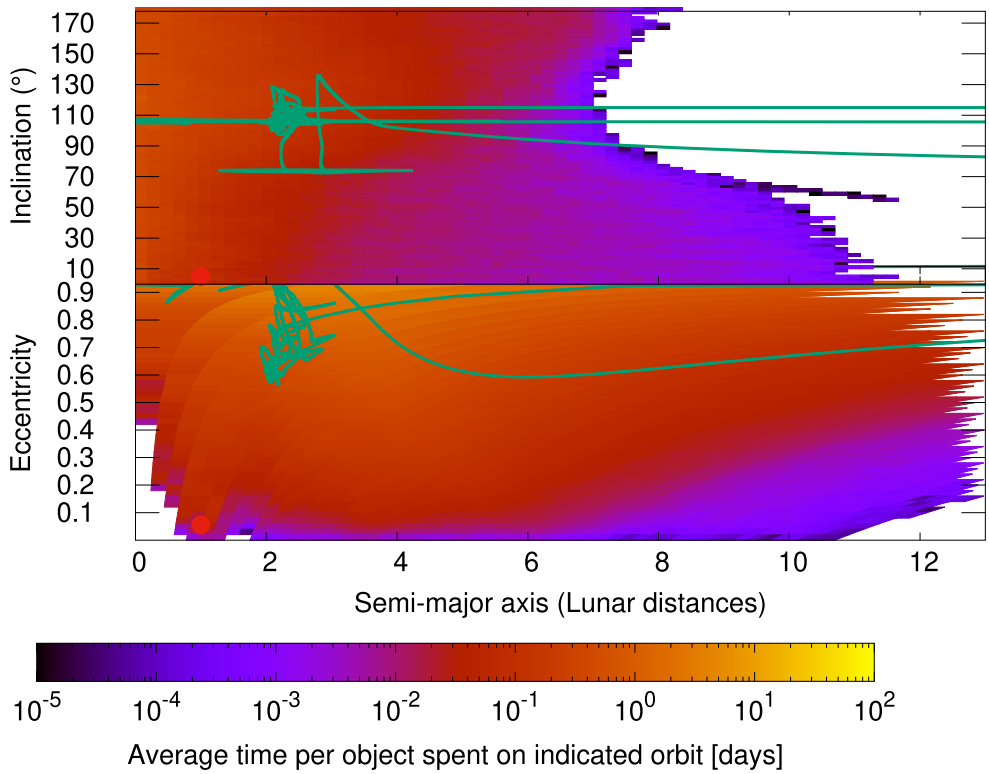

Figure 4. The trajectory of 2020 CD3 in the geocentric (a, i)-space (top) and (a, e)-space (bottom) plotted over the simulated results of the residence time of minimoons. Solid red dot represents the Moon.

uncertainty distribution of solutions #23, #25, and #26 is compatible with multiple VIs with potential impacts starting in 2082 September. The impact probability of the first VI is 1.1% for solution #23 (nominal impact date is 2082 September 8), 3.8% for solution #25 (2082 September 9), and 3.4% for solution #26 (2082 September 9). This is the VI with the highest impact probability for these three solutions. It is followed by a second VI on 2083 February 21 with impact probability 0.1% for all three orbit solutions, and a VI in 2083 June with an impact probability of 0.5%, 0.1%, and 0.1%, respectively. There are VIs almost every year through 2090 and between 2099 and 2120. The cumulative impact probability for solution #23 is 2.8%, 4.9% for solution #25, and 4.4% for solution #26.

Solution #24 is compatible with earlier VIs, the first occurring on 2061 September 14 with an impact probability of 0.2%. We found multiple VIs through 2064 and almost one VI per year between 2077 and 2120. The impact probability of the 2082 September 9 VI is 0.06%, which is 1 order of magnitude smaller than the corresponding VI of solutions #23, #25, and #26. Furthermore, the total cumulative impact probability of solution #24 is 0.9%. It is approximately three times smaller than the other three solutions.

5. Conclusion

Asteroid 2020 CD3 is only the second known minimoon of Earth after asteroid 2006 RH_{120} (Kwiatkowski et al. 2009), which was in a geocentric orbit between 2006 July to 2007 July. Fedorets et al. (2020) showed that 2020 CD3 spent at least 2.5 years orbiting Earth, significantly longer than the capture duration of asteroid 2020 RH_{120}. However, the orbit of 2020 CD3 prior to 2017 September 15 was unknown because its trajectory was quite chaotic under the strong influence of the gravitational forces from the Earth and the Moon, as well as nongravitational forces due to solar radiation. The precovery observations from DECam and CSS allowed us to improve the asteroid's orbit significantly, determine the capture date and mechanism, and analyze its trajectory in the vicinity of the Earth–Moon system. The highly perturbed trajectory required us to use a highly accurate force model, including the full 4×4 gravitational field of the Earth. 2020 CD3 is observable again in March 2044, and could impact Earth sometime after 2061 with a cumulative impact probability of $\gtrsim$1% before 2120.

Part of this research was conducted at the Jet Propulsion Laboratory, California Institute of Technology, under a contract with NASA (80NM0018D0004). G.F. was supported by STFC Grant ST/P000304/1.

ORCID iDs

Shantanu P. Naidu https://orcid.org/0000-0003-4439-7014
Marco Micheli https://orcid.org/0000-0001-7895-8209
Davide Farnocchia https://orcid.org/0000-0003-0774-884X
Javier Roa https://orcid.org/0000-0002-0810-1549
Grigori Fedorets https://orcid.org/0000-0002-8418-4809
Robert Weryk https://orcid.org/0000-0002-0439-9341

References

Bolin, B., Jedicke, R., Granvik, M., et al. 2014, Icar, 241, 280
Bolin, B. T., Fremling, C., Holt, T. R., et al. 2020, ApJL, 900, L45

Chesley, S. R., & Yeomans, D. K. 2005, in IAU Colloq. 197, Dynamics of Populations of Planetary Systems, ed. Z. Knežević & A. Milani (Cambridge: Cambridge Univ. Press), 289
de la Fuente Marcos, C., & de la Fuente Marcos, R. 2020, MNRAS, 494, 1089
Farnocchia, D., Chesley, S. R., Milani, A., Gronchi, G. F., & Chodas, P. W. 2015, Orbits, Long-Term Predictions, Impact Monitoring, 815
Farnocchia, D., Eggl, S., Chodas, P. W., Giorgini, J. D., & Chesley, S. R. 2019, CeMDA, 131, 36
Fedorets, G., Granvik, M., & Jedicke, R. 2017, Icar, 285, 83
Fedorets, G., Micheli, M., Jedicke, R., et al. 2020, AJ, 160, 277
Folkner, W. M., Williams, J. G., Boggs, D. H., Park, R. S., & Kuchynka, P. 2014, IPNPR, 42-196, 1
Granvik, M., Vaubaillon, J., & Jedicke, R. 2012, Icar, 218, 262
Gwyn, S. D. J., Hill, N., & Kavelaars, J. J. 2012, PASP, 124, 579
Jedicke, R., Bolin, B. T., Bottke, W. F., et al. 2018, FrASS, 5, A13
Kwiatkowski, T., Kryszczyńska, A., Polińska, M., et al. 2009, A&A, 495, 967
Lemoine, F., Kenyon, S., Factor, J., et al. 1998, The Development of the Joint NASA GSFC and NIMA Geopotential Model EGM96, NASA Goddard Space Flight Center, Greenbelt, Maryland, 20771 USA, Tech. rep., Report NASA/TP1998-206861
Marsden, B., Sekanina, Z., & Yeomans, D. K. 1973, AJ, 78, 211